Robotica (2005) volume 23, pp. 219–229. © 2005 Cambridge University Press
doi:10.1017/S0263574704000797 Printed in the United Kingdom

Kinematics and inverse dynamics analysis for a general 3-PRS spatial parallel mechanism

Yangmin Li* and Qingsong Xu

Dept. of Electromechanical Engineering, Faculty of Science and Technology,
University of Macau, Av. Padre Tomás Pereira S. J., Taipa, Macao SAR (P. R. of China)
E-mail: ymli@umac.mo

(Received in Final Form: June 15, 2004)

SUMMARY

In this paper, the kinematics and inverse dynamics of a novel kind of mechanism called a general 3-PRS parallel mechanism is investigated. In the kinematics study, the inverse kinematics solution is derived in closed form, and the forward kinematics problem is resolved by the Newton iterative method seeking for an on-line solution to this issue. The inverse dynamics analysis is approached with two methods: Lagrangian formulations and principle of virtual work. After deriving the dynamic model by a Lagrangian formulation approach, the simulation results of two introduced examples quantitatively and qualitatively verify the accuracy of the derived dynamic equations. By introducing a simplifying hypothesis, a simplified dynamic model is set up using principle of virtual work, also a computer simulation is performed on this reduced model. The simulation results demonstrate that the simplified dynamic model is reasonable under such kind of assumptions through comparison with the precise model derived from the Lagrangian formulation. The inverse dynamics analysis provides a sound basis to develop controllers for controlling over a general 3-PRS parallel robot.

KEYWORDS: Parallel mechanism; Kinematics; Inverse dynamics; Simulation.

1. INTRODUCTION

Parallel robots have received increasing attention due to their inherent advantages over conventional serial mechanism, such as high rigidity, high load capacity, high velocity, and high precision. A definite advantage of parallel robots is the fact that, in most cases, actuators can be placed on the truss, thus achieving a limited weight for the moving parts, which makes it possible for parallel robots to move at a high speed. The major drawback of parallel robots is their limited range of motion. Considering the tradeoff between high operational precision and large working volume, parallel actuated mechanisms become ideal devices for applications that require high positional accuracy within a limited workspace.

There are many works concerning 6-DOF parallel robots.[1,2] Although general 6-DOF parallel mechanisms, such as Gough-Stewart platforms, have attracted considerable research interests in the application field of manufacture, in a sense it is not necessary to use 6-DOF in most cases. In recent years, parallel mechanisms with less than 6-DOF have attracted the attention of many researchers. Many 3-DOF parallel manipulators have been designed; extensive research work focused on the famous DELTA robot with three translational DOF,[3] Tsai's manipulator which was similar to DELTA robot but not a version of DELTA,[4] and other 3-RPS parallel mechanisms which were exploited as micromanipulators.[5] The static balancing problem of the 3-RRS spatial parallel mechanisms was discussed by using counter-weights and springs.[6] A new type of 4-DOF parallel robots called H4 was proposed.[7] Although several 3-PRS spatial parallel mechanisms were designed and analyzed,[8,9] and different methods in actuators arrangement in these mechanisms were used, they still could be considered as the same type of mechanisms and be resolved using the same kinematics technique. In addition, although the parallel mechanisms with less DOF have been investigated extensively on a kinematic scope, investigations on their dynamics are relatively few. The dynamic model of a DELTA parallel robot based on the virtual work principle was established.[10] The dynamics of a 3-DOF in-parallel actuated manipulator was analyzed using the Lagrange approach.[11] A dynamic analysis of a 3-PRS mechanism with the actuators perpendicular to the base platform was performed.[12] The inverse dynamics analysis for a novel 3-DOF spatial parallel manipulator using the Newton-Euler method was investigated.[13]

In this paper, we propose a new general type of 3-PRS parallel mechanism by modifying the current existed structure of a 3-PRS parallel mechanism, which will be more suitable for practical applications. The kinematics and dynamics analysis for this general 3-PRS parallel mechanism will become more complicated than the current existed one.[14] Based on our previous research results,[15] we analyze kinematics with constraint conditions and obtain a constrained Jacobian matrix. Hence not only the inverse kinematics problem is resolved in closed form, but also the forward kinematics problem is resolved numerically. The classical Newton iterative method is exploited for seeking an on-line solution to the forward kinematic problem. The key issue in the dynamics analysis is to establish an inverse dynamics model of the parallel manipulator, which can solve

* Corresponding author

https://doi.org/10.1017/S0263574704000797 Published online by Cambridge University Press



Fig. 1. A general 3-PRS parallel mechanism.

the required actuator torques given a desired trajectory of the moving platform. The dynamics of the parallel robots, which is a very important step to design a controller, tends to be very complicated in case of the actuating legs having closed-loop connections with each other. The closed mechanical chains make the dynamics of parallel robots coupled and highly nonlinear.

The rest of the paper is organized as follows: The mechanism is described and the kinematics analysis is presented in Section 2. In Section 3, the dynamic model using Lagrange equation is established. Then, by introducing hypothesis of simplification, the dynamic equations are derived through the principle of virtual work. Two examples are chosen to illustrate the dynamic simulation and verify the accuracy of the derived dynamic models. And the simulation results also show the efficiency of the adopted simplification hypothesis in Section 4. Some conclusions and future research directions are given in Section 5.

2. KINEMATICS ANALYSIS

2.1. Description of a general 3-PRS parallel mechanism

The architecture of a general 3-PRS parallel mechanism is shown in Figure 1, which is composed of a moving platform, a fixed base, and three supporting limbs with identical geometrical structure. Each limb connects the fixed base to the moving platform by a prismatic joint, a revolute joint and a spherical joint in series. A linear actuator actuates the prismatic joint of each limb. Thus, the base is attached to the moving platform by three identical PRS linkages. Since the joint DOF of each limb is equal to five, each limb provides one constraint to the moving platform, hence a 3-PRS mechanism has three DOF, which are two DOF of rotation about two perpendicular axes intersecting at the moving platform center and constructing a horizontal plane, and one DOF of a vertical translated motion.

As shown in Figure 2, a Cartesian reference coordinate frame $O\{x,y,z\}$ is attached at the centered point O of the fixed triangle base platform $\Delta A_1A_2A_3$. And another coordinate frame $P\{u,v,w\}$ is attached on the moving platform at point P which is the centered point of triangle $\Delta B_1B_2B_3$. The x-axis is along $\overrightarrow{OA_1}$ direction, and the u-axis is along $\overrightarrow{PB_1}$ direction. α is defined as the actuator's arrangement angle.

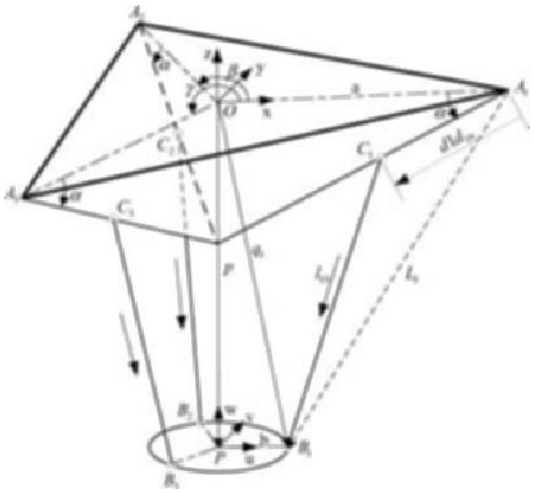


Fig. 2. Schematic representation of a general 3-PRS parallel mechanism.

In this study, we assume that $\beta = 120^\circ$ and $\gamma = 240^\circ$ for brevity. For a general 3-PRS parallel mechanism, let $d = [d_1\ d_2\ d_3]^T$ be a set of the joint space variables. The transformation from the moving platform to the fixed base can be described by a position vector $p = [p_x\ p_y\ p_z]^T$, and a rotation matrix ${}^AR_B$ in $[3 \times 3]$. Let u, v and w be three unit vectors defined along the u, v and w axis of the moving frame $P\{u,v,w\}$ accordingly. Then the rotation matrix can be expressed in terms of the direction cosines of u, v and w as

$$ {}^AR_B = \begin{bmatrix} u_x & v_x & w_x \\ u_y & v_y & w_y \\ u_z & v_z & w_z \end{bmatrix} \tag{1} $$

The orientation of the moving platform can be described by three Euler angles ϕ, θ and ψ, which are angles rotated about z, x, and y axis of the fixed reference frame in sequence, i.e.

$$ \begin{aligned} {}^AR_B &= R_y(\theta)R_x(\psi)R_z(\phi) \\ &= \begin{bmatrix} c\theta c\phi + s\psi s\theta s\phi & -c\theta s\phi + s\psi s\theta c\phi & c\psi s\theta \\ c\psi s\phi & c\psi c\phi & -s\psi \\ -s\theta c\phi + s\psi c\theta s\phi & s\theta s\phi + s\psi c\theta c\phi & c\psi c\theta \end{bmatrix} \end{aligned} \tag{2} $$

where c denotes cosine and s denotes sine. ${}^AR_B$ can also be described by Z-Y-Z Euler angles in terms of θ_1, θ_2, and θ_3. Let ${}^Bb_i$ be the vector from P to B_i, which can be expressed in the moving frame as follows:

$$ \begin{aligned} {}^Bb_1 &= [b \quad 0 \quad 0]^T \\ {}^Bb_2 &= [-b/2 \quad \sqrt{3}\,b/2 \quad 0]^T \\ {}^Bb_3 &= [-b/2 \quad -\sqrt{3}\,b/2 \quad 0]^T \end{aligned} \tag{3} $$

The position vector q_i can be obtained by

$$ q_i = p + {}^AR_B\ {}^Bb_i \tag{4} $$

https://doi.org/10.1017/S0263574704000797 Published online by Cambridge University Press

Substituting Equations (1) and (3) into Equation (4) yields

$$q_1 = \begin{bmatrix} p_x + bu_x \\ p_y + bu_y \\ p_z + bu_z \end{bmatrix}$$

$$q_2 = \begin{bmatrix} p_x - bu_x/2 + \sqrt{3}\, bv_x/2 \\ p_y - bu_y/2 + \sqrt{3}\, bv_y/2 \\ p_z - bu_z/2 + \sqrt{3}\, bv_z/2 \end{bmatrix} \tag{5}$$

$$q_3 = \begin{bmatrix} p_x - bu_x/2 - \sqrt{3}\, bv_x/2 \\ p_y - bu_y/2 - \sqrt{3}\, bv_y/2 \\ p_z - bu_z/2 - \sqrt{3}\, bv_z/2 \end{bmatrix}$$

2.2. Constraint conditions

Considering the mechanical constraints imposed by revolute joints, the spherical joints B_i can only move in the planes defined by vectors d_i and l_i (i.e. the ith actuator and the ith leg). Therefore the following three equations hold

$$q_{1y} = 0 \tag{6}$$

$$q_{2y} = -\sqrt{3}\, q_{2x} \tag{7}$$

$$q_{3y} = \sqrt{3}\, q_{3x} \tag{8}$$

Substituting the components of q_i from Equation (5) into above three equations, yields

$$p_y + b\, u_x = 0 \tag{9}$$

$$v_x = u_y \tag{10}$$

$$p_x = b(u_x - v_y)/2 \tag{11}$$

Hence Equations (9) to (11) impose three constraints on the motion of the moving platform.

2.3. Jacobian matrix analysis

From Figure 2, vector loops of the ith leg can be written as

$$p + b_i = a_i + d_i d_{i0} + l\, l_{i0} \tag{12}$$

where l_{i0} is a unit vector of the ith leg in the direction of $\overrightarrow{C_i B_i}$, d_{i0} represents a unit vector of the ith linear actuator. The three unit vectors can be expressed as

$$\begin{aligned} d_{10} &= [-c\alpha \quad 0 \quad -s\alpha]^T \\ d_{20} &= [c\alpha/2 \quad -\sqrt{3}\, c\alpha/2 \quad -s\alpha]^T \\ d_{30} &= [c\alpha/2 \quad \sqrt{3}\, c\alpha/2 \quad -s\alpha]^T \end{aligned} \tag{13}$$

Vectors a_i in the base platform can be expressed as

$$\begin{aligned} a_1 &= [a \quad 0 \quad 0]^T \\ a_2 &= [-a/2 \quad \sqrt{3}\, a/2 \quad 0]^T \\ a_3 &= [-a/2 \quad -\sqrt{3}\, a/2 \quad 0]^T \end{aligned} \tag{14}$$

Differentiating Equation (12) with respect to time yields

$$\upsilon_p + \omega_p \times b_i = \upsilon_i d_{i0} + l\, \omega_i \times l_{i0} \tag{15}$$

where υ_p is the three-dimensional linear velocity of the moving platform, ω_p is the angular velocity of the moving platform, υ_i represents the ith actuator linear velocity, and ω_i is the 3-dimensional angular velocity of the ith leg. The passive variables ω_i can be eliminated by dot-multiply both sides of Equation (15) with l_{i0}, that is

$$l_{i0} \cdot \upsilon_p + (b_i \times l_{i0}) \cdot \omega_p = \upsilon_i l_{i0} \cdot d_{i0} \tag{16}$$

where "$\cdot$" and "$\times$" represents the dot product and cross product between vectors respectively. Let $\dot{X}_p = \begin{bmatrix} \upsilon_p & \omega_p \end{bmatrix}^T$ and $\dot{d} = [\upsilon_1 \; \upsilon_2 \; \upsilon_3]^T$ be the vector of moving platform velocities and vector of actuator joint rates respectively. The following equation can be derived from Equation (16)

$$J_x\, \dot{X}_p = J_q\, \dot{d} \tag{17}$$

where

$$J_x = \begin{bmatrix} l_{10}^T & (b_1 \times l_{10})^T \\ l_{20}^T & (b_2 \times l_{20})^T \\ l_{30}^T & (b_3 \times l_{30})^T \end{bmatrix}_{3\times 6}$$

$$J_q = \begin{bmatrix} l_{10} \cdot d_{10} & 0 & 0 \\ 0 & l_{20} \cdot d_{20} & 0 \\ 0 & 0 & l_{30} \cdot d_{30} \end{bmatrix}_{3\times 3}$$

When the mechanism is away from singularity, we have

$$\dot{d} = J\, \dot{X}_p \tag{18}$$

where $J = J_q^{-1} J_x$ is a matrix in $[3 \times 6]$. Equation (18) represents the inverse velocity solution of a general 3-PRS parallel mechanism.

The constraint equations (9)–(11) can be detailed as

$$p_y + b\, c\psi s\phi = 0 \tag{19}$$

$$-c\theta s\phi + s\psi s\theta c\phi = c\psi s\phi \tag{20}$$

$$p_x = \frac{b}{2}(c\theta c\phi + s\psi s\theta s\phi - c\psi c\phi) \tag{21}$$

Equations (19) and (20) yield

$$p_y = -b\, c\psi s\phi \tag{22}$$

$$\phi = \tan^{-1}\left(\frac{s\psi s\theta}{c\psi + c\theta}\right) \tag{23}$$

Let p_z, ψ and θ be specified independent variables. Substitution of these three values into Equations (21)–(23) can calculate the constrained variables p_x, p_y and ϕ. Let $\dot{X} = [\upsilon_{pz} \; \omega_{px} \; \omega_{py}]^T$, then

$$\dot{X}_p = G\, \dot{X} \tag{24}$$

https://doi.org/10.1017/S0263574704000797 Published online by Cambridge University Press

where

$$G = \begin{bmatrix} \frac{\partial p_x}{\partial p_z} & \frac{\partial p_x}{\partial \psi} & \frac{\partial p_x}{\partial \theta} \\ \frac{\partial p_y}{\partial p_z} & \frac{\partial p_y}{\partial \psi} & \frac{\partial p_y}{\partial \theta} \\ 1 & 0 & 0 \\ 0 & 1 & 0 \\ 0 & 0 & 1 \\ \frac{\partial \phi}{\partial p_z} & \frac{\partial \phi}{\partial \psi} & \frac{\partial \phi}{\partial \theta} \end{bmatrix}$$

Therefore

$$\dot{d} = J_c \, \dot{X} \tag{25}$$

where $J_c = JG$ is a Jacobian matrix in $[3 \times 3]$ which includes the effect of the mechanical constraints on the mechanism. J_c is defined as the constrained Jacobian matrix of a general 3-PRS parallel mechanism.

2.4. Inverse kinematics analysis

The inverse kinematics problem resolves the actuated variables from a given position and orientation of the output platform. From Figure 2, we can obtain

$$L_i = d_i d_{i0} + l \, l_{i0} \tag{26}$$

$$L_i = q_i - a_i \tag{27}$$

where q_i is expressed by Equation (4). Since p and ${}^{A}R_{B}$ are known values, L_i is also known.

Equaiton (26) yields

$$L_i - d_i d_{i0} = l \, l_{i0} \tag{28}$$

Squaring both sides of Equation (28) and rearranging it yields

$$d_i^2 - 2 d_i L_i \cdot d_{i0} + L_i^2 - l^2 = 0 \tag{29}$$

Solving Equation (29), the inverse kinematics solutions can be derived as

$$d_i = (L_i \cdot d_{i0}) \pm \sqrt{(L_i \cdot d_{i0})^2 - L_i^2 + l^2} \tag{30}$$

We can see that there exist two solutions for each actuator, there are eight possible solutions totally for a given platform position and orientation. In this paper, only the negative square root is selected as a solution in case of the three legs are inclined inward from top to bottom.

2.5. Forward kinematics analysis

Given a set of actuated inputs, the position and orientation of the output platform is resolved by the forward kinematics. The forward kinematic problem can be resolved by non-linear equations solving method.

Let φ_i be measured from $\overrightarrow{C_i B_i}$ to the fixed base platform, then the three vectors q_1, q_2 and q_3 can also be expressed as:

$$q_1 = \begin{bmatrix} a - d_1 c\alpha - l c\varphi_1 \\ 0 \\ -d_1 s\alpha - l s\varphi_1 \end{bmatrix}$$

$$q_2 = \begin{bmatrix} -(a - d_2 c\alpha - l c\varphi_2)/2 \\ \sqrt{3}\,(a - d_2 c\alpha - l c\varphi_2)/2 \\ -d_2 s\alpha - l s\varphi_2 \end{bmatrix} \tag{31}$$

$$q_3 = \begin{bmatrix} -(a - d_3 c\alpha - l c\varphi_3)/2 \\ -\sqrt{3}\,(a - d_3 c\alpha - l c\varphi_3)/2 \\ -d_3 s\alpha - l s\varphi_3 \end{bmatrix}$$

The geometric distance between two spherical joints B_i and B_j $(i \neq j)$ is equal to a constant, that is $\|B_i B_j\| = \sqrt{3} b$ $(i \neq j)$. We can obtain three equations as follows:

$$[q_i - q_{i+1}]^T \, [q_i - q_{i+1}] - 3b^2 = 0 \tag{32}$$

That is

$$\begin{aligned} e_{1i} c\varphi_i c\varphi_{i+1} + e_{2i} s\varphi_i s\varphi_{i+1} + e_{3i} c\varphi_i + e_{4i} s\varphi_i \\ + e_{5i} c\varphi_{i+1} + e_{6i} s\varphi_{i+1} + e_{7i} = 0 \end{aligned} \tag{33}$$

where $e_{1i} = l^2$, $e_{2i} = -2l^2$, $e_{3i} = [(2d_i + d_{i+1})c\alpha - 3a]l$, $e_{4i} = 2l(d_i - d_{i+1})s\alpha$, $e_{5i} = [(d_i + 2d_{i+1})c\alpha - 3a]l$, $e_{6i} = -2l(d_i - d_{i+1})s\alpha$, $e_{7i} = (d_i - d_{i+1})^2 + 3d_i d_{i+1} c^2\alpha - 3a(d_i + 2d_{i+1})c\alpha + 3(a^2 - b^2) + 2l^2$, $i = 1, 2, 3$.

Substituting the trigonometric identities $s\varphi_i = \frac{2t_i}{1+t_i^2}$ and $c\varphi_i = \frac{1-t_i^2}{1+t_i^2}$ $(t_i = \tan\frac{\varphi_i}{2})$ into Equation (33) yields three fourth-degree polynomials in t_1, t_2, and t_3:

$$\begin{aligned} \Re_{1i} t_i^2 t_{i+1}^2 + \Re_{2i} t_i t_{i+1}^2 + \Re_{3i} t_i^2 t_{i+1} + \Re_{4i} t_i^2 + \Re_{5i} t_{i+1}^2 \\ + \Re_{6i} t_i t_{i+1} + \Re_{7i} t_i + \Re_{8i} t_{i+1} + \Re_{9i} = 0 \end{aligned} \tag{34}$$

where $\Re_{1i} = e_{1i} - e_{3i} - e_{5i} + e_{7i}$, $\Re_{2i} = 2e_{4i}$, $\Re_{3i} = 2e_{6i}$, $\Re_{4i} = -e_{1i} - e_{3i} + e_{5i} + e_{7i}$, $\Re_{5i} = -e_{1i} + e_{3i} - e_{5i} + e_{7i}$, $\Re_{6i} = 4e_{2i}$, $\Re_{7i} = 2e_{4i}$, $\Re_{8i} = 2e_{6i}$, $\Re_{9i} = e_{1i} + e_{3i} + e_{5i} + e_{7i}$, i=1, 2, 3.

By applying Bezout's elimination method, the entire system equation can be reduced to a 16th-degree polynomial in single variable.[14] Tsai et al.[9] solved the three angles φ_1, φ_2 and φ_3 for a 3-PRS parallel mechanism in case of three actuator rails parallel to one another and perpendicular to the base platform using Bezout's elimination method and an optimization technique. The three angles φ_1, φ_2 and φ_3 for a general 3-PRS parallel mechanism can also be solved by the same methods. Once φ_1, φ_2 and φ_3 are solved, the position vector of the moving platform is obtained by

$$p = \frac{1}{3}(q_1 + q_2 + q_3) \tag{35}$$

https://doi.org/10.1017/S0263574704000797 Published online by Cambridge University Press

Table I. Parameters of a general 3-PRS parallel mechanism.

Parameter	Value
a	400 mm
b	200 mm
l	550 mm
m_p	1.0 kg
m_s	0.2 kg
m_l	0.2 kg
g	0.98 m/s^2

Components of rotation matrix ${}^A R_B$ can be found by

$$u = \frac{q_1 - p}{b} \tag{36}$$

$$v = \frac{q_2 - q_3}{\sqrt{3}b} \tag{37}$$

$$w = u \times v \tag{38}$$

Then Euler angles ψ, θ and ϕ can be solved easily.

In this paper, the forward kinematic problem is resolved numerically by the classical Newton iterative method. For a certain poses of the general 3-PRS parallel mechanism, a system with three equations can be written as

$$f(p_z, \psi, \theta) = d(p_z, \psi, \theta) - d_{given} = 0 \tag{39}$$

where $d(p_z, \psi, \theta)$ is the joint space coordinate vector generated from the inverse kinematic solution, and d_{given} is the known joint space coordinate vector which can be measured.

Let X^n denote a given set $(p_z^n, \psi^n, \theta^n)$, then the following equation holds according to the Newton iterative method

$$X^{k+1} = X^k - \left(\frac{\partial f(X^k)}{\partial X}\right)^{-1} f(X^k) \tag{40}$$

Applying $\frac{\partial f(X^k)}{\partial X} = J_c(X^k)$, Equation (40) can be written as

$$X^{k+1} = X^k - (J_c(X^k))^{-1}(d(X^k) - d_{given}) \tag{41}$$

Starting with an initial estimated value X^0, the iterative process will end once the maximum of the absolute value of $d(X^k) - d_{given}$ is less than a specified tolerance. Since there are many solutions, it is necessary to start with an initial guess closed to the actual pose of the moving platform. Such an initial guess can be chosen by either the known desired pose or the pose of a previous point on the trajectory at a short time interval in the past.

A computer program is developed to implement the Newton iterative method. For the kinematic parameters of a general 3-PRS parallel mechanism shown in Table I, let the moving platform be in the Cartesian pose

$$[p_z \quad \psi \quad \theta]^T = [-470 \quad 0.4 \quad -0.3]^T \tag{42}$$

Table II. Results of the forward kinematics analysis using Newton iterative method.

	p_z (mm)	ψ (rad)	θ (rad)
0	−468	0.35	−0.25
1	−470.129683164667	0.400795016562	−0.298155481458
2	−470.000294997604	0.399999621592	−0.299997609967
3	−469.999988966593	0.400000066234	−0.300000149838
4	−469.999988966119	0.400000066232	−0.300000149846

Then the constrained variables can be derived by Equations (21)–(23).

$$\begin{bmatrix} p_x & p_y & \phi \end{bmatrix}^T = [4.1256 \quad 11.2767 \quad -0.0613]^T \tag{43}$$

where the unit of linear displacement is mm and the unit of angular displacement is rad.

The joint space coordinate vector can be derived from the inverse kinematics solution

$$[d_1 \quad d_2 \quad d_3]^T = [-101.4888 \quad -91.8057 \quad 80.5667]^T \tag{44}$$

where all units of the joint lengths are mm. We assume that d_{given} is given by Equation (44), which may be measured from joint space, and we need to find an approximate numerical solution for X. Applying the numerical technique presented above with an initial guess of the following equation

$$X^0 = (-468, \quad 0.35, \quad 0.25) \tag{45}$$

and a specified tolerance 1e-6 as the stopping criterion, the convergence is reached after four iterations as shown in Table II.

3. INVERSE DYNAMICS ANALYSIS USING LAGRANGIAN FORMULATION

In this section, we focus on the dynamic modeling of a general 3-PRS parallel mechanism using the Lagrange method. For the inverse dynamics problem, the time history of a desired trajectory is given and the problem is to determine the forces of actuators and/or torques required to produce that motion.

The first type of Lagrange's equations is applicable to mechanical systems with either holonomic or nonholonomic constraints. The constraint equations and their first and second derivatives must be involved into the equations of motion to produce a number of equations in accordance with the number of unknowns. In this regard, Lagrange's equations of the first type are more suitable for modeling the dynamics of parallel manipulators, which are complicated in case of the existence of multiple closed-loop chains.[14] Theoretically, the dynamic analysis can be accomplished by using just three generalized coordinates since a general 3-PRS parallel mechanism has 3 DOF. However, this will lead to a cumbersome expression for the Lagrange function due to the complex kinematics of the mechanism. Instead, the first type of Lagrange's equations introduce three redundant coordinates φ_1, φ_2 and φ_3. Thus we have φ_1, φ_2, φ_3, d_1,

https://doi.org/10.1017/S0263574704000797 Published online by Cambridge University Press

d_2 and d_3 as the generalized coordinates. To derive the dynamic equations of a general 3-PRS parallel mechanism, the kinetic and potential energies for all components of the mechanism must be expressed in terms of the chosen generalized coordinates and their derivatives.

3.1. Constraint equations

The constraint equations are obtained from the fact that the distance between two adjacent spherical joints equals to $\sqrt{3}\,b$, i.e.

$$\begin{aligned}\Gamma_i &= \|B_i B_{i+1}\|^2 - 3b^2 \\ &= [q_i - q_{i+1}]^T\,[q_i - q_{i+1}] - 3b^2 \\ &= 0, \quad (i = 1,\ 2 \text{ and } 3)\end{aligned} \tag{46}$$

3.2. Kinetic energy expression

The kinetic energy of the moving platform can be expressed as

$$K_p = K_{Tp} + K_{Rp} \tag{47}$$

where K_{Tp} and K_{Rp} represents translational and rotational kinetic energy respectively. Let m_p represents the mass of the moving platform, then we have

$$K_{Tp} = \frac{1}{2}\, m_p\, v_p^2 \tag{48}$$

where $v_p = \dot{p} = [\dot{p}_x\ \ \dot{p}_y\ \ \dot{p}_z]^T$ is the linear velocity of the moving platform. Let $S = \dot{R}R^{-1}$, where R denotes the rotation matrix ${}^A R_B$, then

$$S = \begin{bmatrix} 0 & -\omega_{pz} & \omega_{py} \\ \omega_{pz} & 0 & -\omega_{px} \\ -\omega_{py} & \omega_{px} & 0 \end{bmatrix} \tag{49}$$

From Equation (49) we can get the angular velocity of the moving platform

$$\omega_p = [\omega_{px} \quad \omega_{py} \quad \omega_{pz}]^T \tag{50}$$

Thus the rotational kinetic energy can be expressed as

$$K_{Rp} = \frac{1}{2}\, \omega_p^T\, I_p\, \omega_p \tag{51}$$

where I_p represents the inertial matrix of the moving platform with respect to the fixed reference frame, and it can be expressed as

$$I_p = R\, I'_p\, R^T \tag{52}$$

where I'_p is the inertial matrix of the moving platform with respect to the moving coordinate $P\{u, v, w\}$, and can be derived by

$$I'_p = m_p \begin{bmatrix} \frac{b^2}{4} & 0 & 0 \\ 0 & \frac{b^2}{4} & 0 \\ 0 & 0 & \frac{b^2}{4} \end{bmatrix} \tag{53}$$

The kinetic energy of three links is

$$K_l = \sum_{i=1}^{3} (K_{Tli} + K_{Rli}), \quad (i = 1,\ 2,\ \text{and } 3) \tag{54}$$

where K_{Tli} and K_{Rli} represents the translational and rotational kinetic energy of the ith link, respectively. Let ω_{li} represents the angular velocity of the ith link, then

$$K_{Rli} = \frac{1}{2}\, \omega_{li}^T\, I_{li}\, \omega_{li}, \quad (i = 1,\ 2,\ \text{and } 3) \tag{55}$$

where $I_{li} = \frac{1}{12} m_l l^2$ denotes the rotational inertia of the ith link about its mass center, here m_l is the mass of each link. And the three angular velocities can be expressed as

$$\begin{aligned}\omega_{l1} &= \dot{\varphi}_1[0 \quad -1 \quad 0]^T \\ \omega_{l2} &= \dot{\varphi}_2[\sqrt{3}/2 \quad 1/2 \quad 0]^T \\ \omega_{l3} &= \dot{\varphi}_3[-\sqrt{3}/2 \quad 1/2 \quad 0]^T\end{aligned} \tag{56}$$

The translational kinetic energy of the ith link can be expressed as

$$K_{Tli} = \frac{1}{2}\, m_l\, v_{li}^2, \quad (i = 1,\ 2,\ \text{and } 3) \tag{57}$$

where $v_{li} = \dot{d}_i + \frac{l}{2}(\omega_{li} \times l_{i0})$ is the linear velocity of the mass center of the ith link. The kinetic energy of the three sliders is

$$K_s = \sum_{i=1}^{3} \left(\frac{1}{2}\, m_s\, \dot{d}_i^2 \right) \tag{58}$$

where m_s denotes the mass of each slider. Therefore, the total kinetic energy of all components is given by

$$K = K_p + K_l + K_s \tag{59}$$

3.3. Potential energy expression

The total potential energy is derived by

$$\begin{aligned}P = m_p\, g\, p_z &+ \sum_{i=1}^{3} (-m_l\, g\, d_i\, s\alpha) \\ &+ \sum_{i=1}^{3} (-m_s\, g(d_i\, s\alpha + l\, s\varphi_i))\end{aligned} \tag{60}$$

where g is the gravity acceleration.

3.4. Lagrangian formulation

The Lagrange function is defined as

$$L = K - P \tag{61}$$

https://doi.org/10.1017/S0263574704000797 Published online by Cambridge University Press

Therefore the Lagrangian equations of motion can be derived by the six generalized coordinates and their derivatives

$$\frac{d}{dt}\left(\frac{\partial L}{\partial \dot{q}_j}\right) - \frac{\partial L}{\partial q_j} = Q_j + \sum_{i=1}^{k} \lambda_i \frac{\partial \Gamma_i}{\partial q_j}, \quad (i = 1,\ 2, \ldots, 6) \tag{62}$$

where

$$q_j = \begin{cases} \varphi_j & j = 1,\ 2,\ 3 \\ d_{j-3} & j = 4,\ 5,\ 6 \end{cases}$$

$$Q_j = \begin{cases} T_j & j = 1,\ 2,\ 3 \\ F_{j-3} & j = 4,\ 5,\ 6 \end{cases}$$

in which T_j $(j = 1,\ 2,\ 3)$ denotes the frictional torque of the ith link and F_j $(j = 4,\ 5,\ 6)$ represents the actuating force along the direction of the ith slider. In the following discussion, we assume the frictional torque is zero.

For $j = 1$, 2, and 3, we have

$$\lambda_1 \frac{\partial \Gamma_1}{\partial \varphi_j} + \lambda_2 \frac{\partial \Gamma_2}{\partial \varphi_j} + \lambda_3 \frac{\partial \Gamma_3}{\partial \varphi_j} = \frac{d}{dt}\left(\frac{\partial L}{\partial \dot{\varphi}_j}\right) - \frac{\partial L}{\partial \varphi_j} \tag{63}$$

For $j = 4$, 5, and 6, we have

$$F_{j-3} = \frac{d}{dt}\left(\frac{\partial L}{\partial \dot{d}_{j-3}}\right) - \frac{\partial L}{\partial d_{j-3}} - \lambda_1 \frac{\partial \Gamma_1}{\partial d_{j-3}} - \lambda_2 \frac{\partial \Gamma_2}{\partial d_{j-3}} - \lambda_3 \frac{\partial \Gamma_3}{\partial d_{j-3}} \tag{64}$$

Equations (63) form a set of three linear equations in three unknowns from which the three Lagrange multipliers can be determined. Once the Lagrange multipliers are found, the actuator forces can be solved from the second group of Equations (64).

3.5. Dynamic simulations

Although it is more practical to assume the mechanism has two orientation DOF in addition to a third DOF in the z-axis direction, it is possible that the Cartesian coordinates of the centered point of the moving platform can be controlled at a sacrifice of orientation DOF, which can be illustrated by the following two cases.

The rotation matrix can be expressed compactly with three Euler angles in terms of Z-Y-Z Euler angles θ_1, θ_2 and θ_3. The three constraint Equations (9)–(11) yield

$$p_x = -\frac{b}{2}(1 - c\theta_2)\, c(2\theta_1) \tag{65}$$

$$p_y = \frac{b}{2}(1 - c\theta_2)\, s(2\theta_1) \tag{66}$$

$$\theta_3 = -\theta_1 \tag{67}$$

which denote the relations between the constraint and unconstraint variables.

The following dynamic simulations are implemented using *Mathematica* software and animations of results are performed with Matlab software. The architecture and dynamic parameters of the general 3-PRS parallel mechanism is given in Table I.

Case 1:

In the first example, we let the moving platform move straight along z-axis at a constant speed of 5 mm/s, that is

$$p_x = 0$$
$$p_y = 0$$
$$p_z = z0 - 5t$$
$$\theta_1 = 0$$
$$\theta_2 = 0$$
$$\theta_3 = 0$$

where z_0 denotes the initial position of the center of the moving platform in z-axis direction, and t is the time variable. We assume that $z_0 = -460$ mm, which is within the workspace. One simulation result is shown in Figure 3 in case of

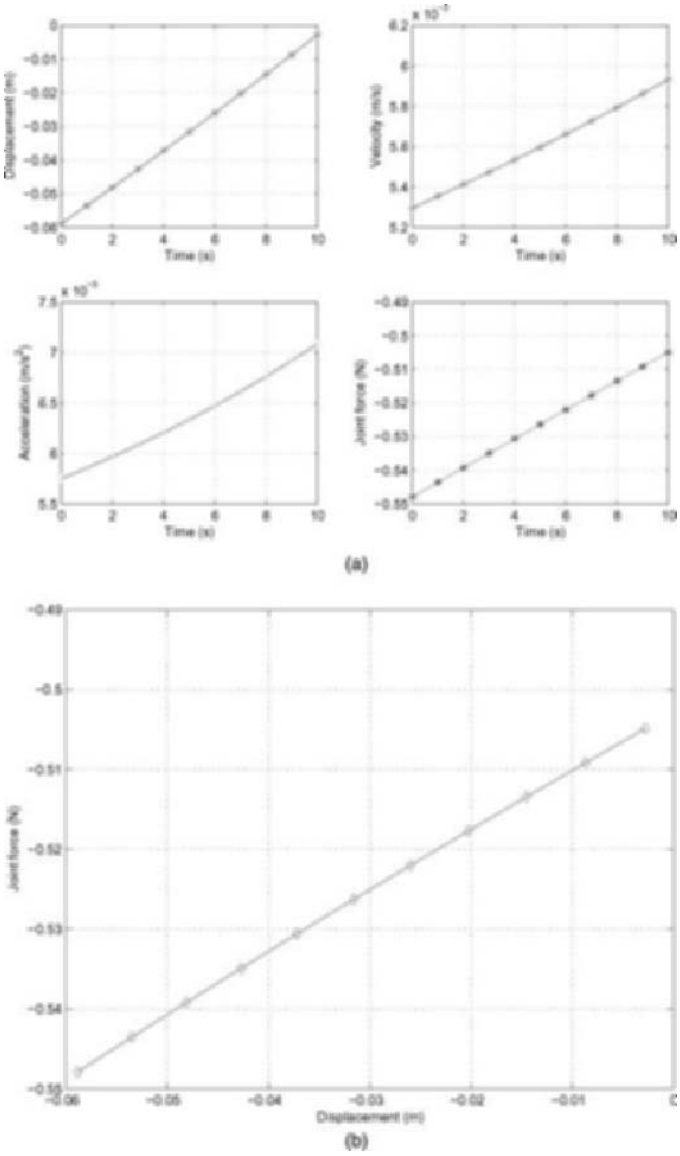


Fig. 3. Simulation results of case 1 when $\alpha = 30°$. (a) Time history of joint displacement, velocity, acceleration and force; (b) Joint force versus joint displacement.

https://doi.org/10.1017/S0263574704000797 Published online by Cambridge University Press

Table III. The actuated work and total energy net increments at various actuator layout angles.

$\alpha\,(deg.)$	$W_a\,(J)$	$\Delta P\,(J)$	$\Delta K\,(J)$	$\Delta U\,(J)$	$\delta W_a\,(\%)$
0	−0.0644462	−0.0637000	3.80660e−5	−0.0636619	1.23198
15	−0.0797426	−0.0795218	8.88762e−6	−0.0795129	0.28888
30	−0.0884876	−0.0884112	3.01750e−6	−0.0884082	0.08981
45	−0.0944654	−0.0944392	1.21395e−6	−0.0944380	0.02901
60	−0.0992081	−0.0992009	4.83338e−7	−0.0992004	0.00776
75	−0.1034800	−0.1034790	1.31424e−7	−0.1034790	0.00097
90	−0.1078000	−0.1078000	0	−0.1078000	0
105	−0.1126840	−0.1126860	2.86026e−7	−0.1126860	−0.00177
120	−0.1188250	−0.1188490	2.52781e−6	−0.1188470	−0.01851

$\alpha = -30^\circ$. From Figure 3, we can see that the three joint displacements, velocities, accelerations, and joint forces (the negative signs mean that the actuator forces are along the direction of $-d_{i0}$) are identical since the symmetric structure of the mechanism. From viewpoint of energy conservation, the work done by three actuators W_a equals to the increments of total energy of the system ΔU that can be expressed by the kinetic and potential energy ΔK and ΔP, i.e.

$$\begin{aligned}\Delta U &= V_2 - V_1 = (K_2 + P_2) - (K_1 + P_1) \\ &= (P_2 - P_1) + (K_2 - K_1) = \Delta P + \Delta K \end{aligned} \quad (68)$$

From Figure 3(b) we can see that the relation between joint force and displacement is approximately linear, therefore, the approximated value of the work done by the three actuators can be expressed as

$$W_a \approx \frac{1}{2}\,(F_{max} + F_{min})\,(d_{max} - d_{min}) \quad (69)$$

At different actuator layout angles, the corresponding W_a and ΔU are listed in Table III.

From Table III, we can see that there is a little deviation between W_a and ΔU, which is described by

$$\delta W_a = [(W_a - \Delta U)/\Delta U] \times 100\%$$

The deviation partly comes from the fact that the relationship between joint force and displacement is not linear actually. But we notice that when $\alpha = 90^\circ$, W_a equals to ΔU exactly, the simulation result is shown in Figure 4 when $\alpha = 90^\circ$. We can see that the three actuator forces are constants in terms of F_m during the moving platform moves at a constant velocity, so the work done by three actuators exactly equals to

$$W_a = F_m\,(d_{max} - d_{min}) \quad (70)$$

Therefore, the deviation between W_a and ΔU is zero. This simulation results verify partially the accuracy of the derived dynamic equations quantitatively.

Case 2:

In the second example, we let the moving platform track a helical path with the radius of r and the pitch h. The equation

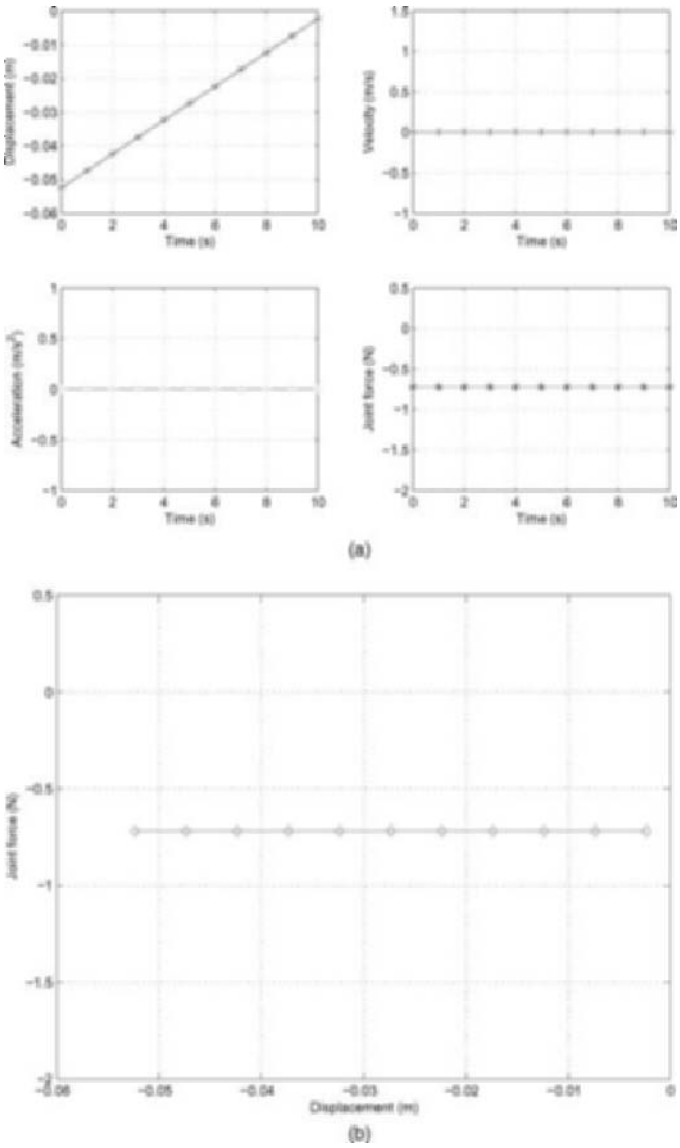


Fig. 4. Simulation results of case 1 when $\alpha = 90^\circ$. (a) Time history of joint displacement, velocity, acceleration and force; (b) Joint force versus joint displacement.

of the helical path with respect to the fixed frame is given by

$$\begin{aligned} x &= r\,\sin(\eta t) \\ y &= r\,\cos(\eta t) \\ z &= z0 + \frac{h}{H}\,t \end{aligned} \quad (71)$$

https://doi.org/10.1017/S0263574704000797 Published online by Cambridge University Press

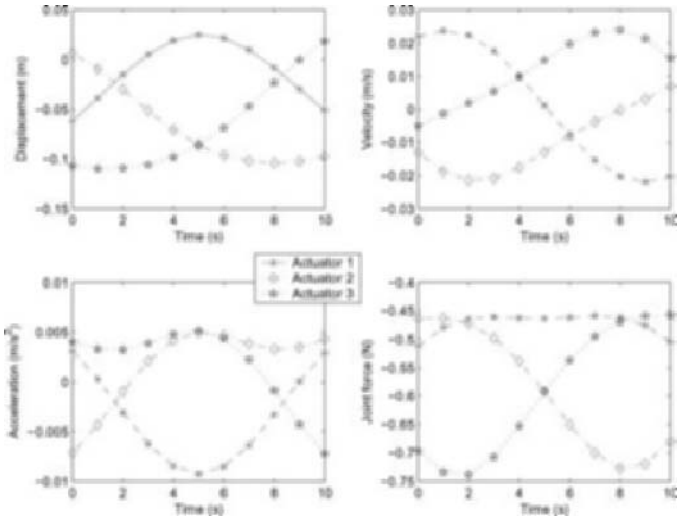


Fig. 5. Simulation results of case 2: time history of joint displacement, velocity, acceleration and force.

Table IV. The increments of total energy at different actuator layout angles.

α (*deg.*)	ΔU (J)
0	−0.0126433
15	−0.0157012
30	−0.0174660
45	−0.0187225
60	−0.0197393
75	−0.0206545
90	−0.0215600
105	−0.0225364
120	−0.0236818

where T is the time required to travel one pitch, η is the angular frequency, and t is the time variable. We assume that $z0 = -460$ mm, $r = 5$ mm, $h = 10$ mm, $\eta = \frac{\pi}{5}$ rad/s, and $T = 10$ s.

Substituting equation (71) into Equations (65) and (66) yields

$$2\theta_1 + \eta t = n\pi, \quad n = 0, \pm 1, \ldots$$
$$\cos(\theta_2) = 1 - \frac{2r}{b}$$

Hence we can obtain

$$\theta_1 = -\frac{1}{2}\eta t + \frac{\pi}{2}$$
$$\theta_2 = \cos^{-1}\left(1 - \frac{2r}{b}\right)$$
$$\theta_3 = -\theta_1$$

The simulation results in case of the actuator layout angle $\alpha = 30^\circ$ are shown in Figure 5. As the actuator layout angle is changed, the increment of total energy ΔU(the work done by actuators) is shown in Table IV. The ranges of actuator displacements and joint forces versus actuator layout angles are shown in Figure 6 and 7, respectively.

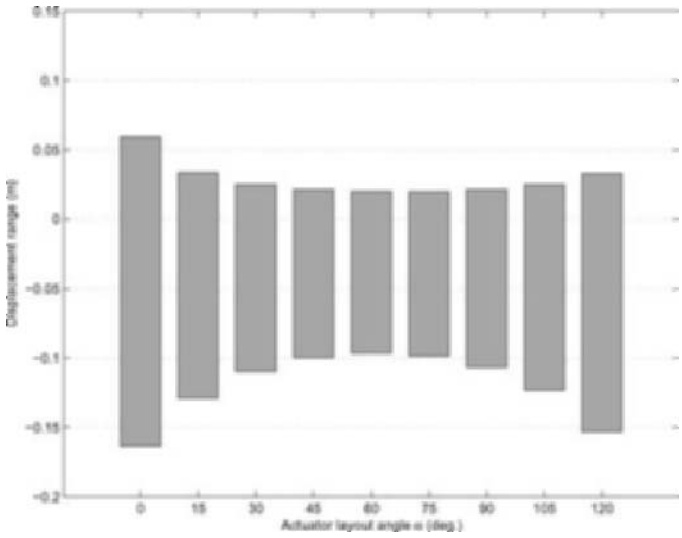


Fig. 6. The range of actuator displacements versus actuator layout angles.

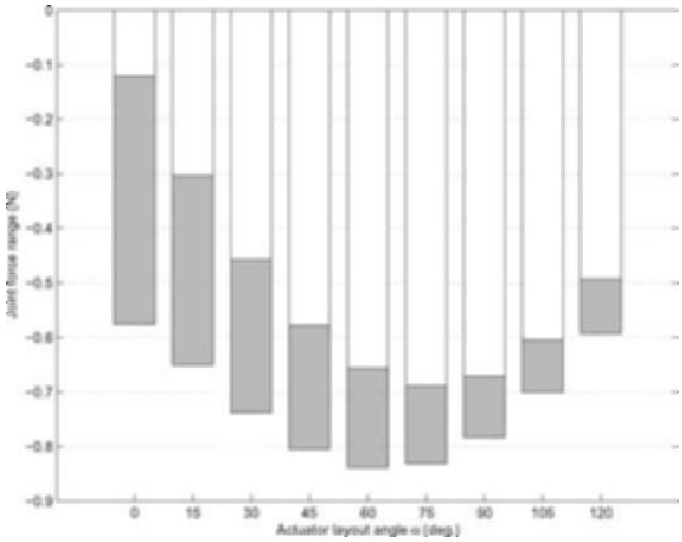


Fig. 7. The range of actuator forces versus actuator layout angles.

When tracking the same helical path, we can see from Table IV that the work done by actuators at various actuators layout angles is almost equivalent. From Figure 6 we can see that the actuators can move within the minimum motion range when the actuator layout angle is around 60°, but it needs the maximum values of actuated force at the same time, which can be observed from Figure 7. This can be explained from the viewpoint of work that is a product of force and the corresponding displacement, that is, while doing the identical work, the smaller displacement requires the larger force. The simulation results verify the accuracy of the derived dynamic equations qualitatively.

4. DYNAMICS MODELING WITH PRINCIPLE OF VIRTUAL WORK

4.1. Simplifying hypothesis

For a general 3-PRS parallel mechanism, the complexity of the dynamic model partly comes from the three moving legs.

https://doi.org/10.1017/S0263574704000797 Published online by Cambridge University Press

We can simplify the dynamic problem by neglecting their rotational inertias according to the following simplifying hypotheses: The rotational inertias of legs are neglected. The masses of legs are optimally divided into two portions and placed at their two extremities, i.e. 1/2 at its upper extremity (slider) and 1/2 at its lower extremity (moving platform). Then, the equivalent mass of the slider and the moving platform can be written as

$$\hat{m}_s = m_s + \frac{1}{2} m_l, \quad \hat{m}_p = m_p + \frac{3}{2} m_l.$$

4.2. Dynamic modeling

From the kinematics analysis, we know that the constrained Jacobian matrix of a general 3-PRS parallel mechanism is J_c, which is a 3×3 matrix and describes the relation between the actuators velocity and the derivatives of dependent variables of the moving platform. From Equation (25) we can generate

$$\delta X = J_c^{-1} \delta d \tag{72}$$

Let $f = [f_1 \ f_2 \ f_3]^T$ be the actuator force vector, and $\delta d = [\delta d_1 \ \delta d_2 \ \delta d_3]^T$ be the corresponding virtual displacement vector. Let $F_a = [F_x \ F_y \ F_z \ N_x \ N_y \ N_z]^T$ be the external forces actuated on the moving platform. Since a general 3-PRS parallel mechanism has three DOF, the moving platform can only bears the forces $F = [F_z \ N_x \ N_y]^T$, which are a subset of F_a, while the other components of F_a are supported by the passive joint bearings. Assume that $\delta X = [\delta p_z \ \delta\theta_x \ \delta\theta_y]^T$ be the corresponding virtual displacement vectors. Then by adopting the principle of virtual work, the following equation can be derived

$$f^T \delta d + G_s^T \delta d + F^T \delta X + G_p^T \delta X - f_s^T \delta d - f_p^T \delta X = 0 \tag{73}$$

where $G_s = [\hat{m}_s g \sin(\alpha) \quad \hat{m}_s g \sin(\alpha) \quad \hat{m}_s g \sin(\alpha)]^T$ represents the gravity force of the sliders, $G_p = [\hat{m}_p g \ 0 \ 0]^T$ is the gravity force of the moving platform, $f_s = [\hat{m}_s \ddot{d}_1 \quad \hat{m}_s \ddot{d}_2 \quad \hat{m}_s \ddot{d}_3]^T$ is the inertial force of the sliders.

The inertial force vector of the moving platform is expressed as

$$f_p = \begin{bmatrix} \hat{m}_p \ddot{p}_z & 0 \\ 0 & \hat{I}_{xy} \begin{bmatrix} \ddot{\theta}_x \\ \ddot{\theta}_y \end{bmatrix} \end{bmatrix}$$

where $\hat{I}_{xy}$ denotes the top-left 2×2 sub-matrix of inertial matrix $\hat{I}_p$ of the moving platform, which can be expressed by replacing m_p in Equation (52) with $\hat{m}_p$.

Substituting Equation (72) into (73) yields

$$\left(f^T + G_s^T + F^T J_c^{-1} + G_p^T J_c^{-1} - f_s^T - f_p^T J_c^{-1}\right) \delta d = 0 \tag{74}$$

Since this equation holds for any virtual displacement δd, we can get

$$f^T + G_s^T + F^T J_c^{-1} + G_p^T J_c^{-1} - f_s^T - f_p^T J_c^{-1} = 0 \tag{75}$$

Taking the transpose of Equation (75) and rearranging it yields

$$f = f_s + \left(J_c^{-1}\right)^T f_p - G_s - \left(J_c^{-1}\right)^T G_p - \left(J_c^{-1}\right)^T F \tag{76}$$

Substituting the inertial forces into Equation (76) yields

$$f = M_s \ddot{d} + \left(J_c^{-1}\right)^T M_p \ddot{X} - G_s - \left(J_c^{-1}\right)^T G_p - \left(J_c^{-1}\right)^T F \tag{77}$$

where

$$M_s = \begin{bmatrix} \hat{m}_s & 0 & 0 \\ 0 & \hat{m}_s & 0 \\ 0 & 0 & \hat{m}_s \end{bmatrix}, \quad M_p = \begin{bmatrix} \hat{m}_p & 0 \\ 0 & \hat{I}_{xy} \end{bmatrix}.$$

From Equation (25), we can get

$$\dot{X} = (J_c)^{-1} \dot{d} \tag{78}$$

Differentiate Equation (78) with respect to time yields

$$\ddot{X} = (J_c)^{-1} \ddot{d} + (\dot{J}_c)^{-1} \dot{d} \tag{79}$$

Substituting Equation (79) into (77), and assuming that there are no external forces, which leads to

$$\begin{aligned} f = &\left[M_s + \left(J_c^{-1}\right)^T M_p \left(J_c^{-1}\right) \ddot{X}\right] \ddot{d} \\ &+ \left[\left(J_c^{-1}\right)^T M_p \left(J_c^{-1}\right)\right] \dot{d} - G_s - \left(J_c^{-1}\right)^T G_p \end{aligned} \tag{80}$$

Equation (80) represents the inverse dynamics equation of a general 3-PRS parallel mechanism generated by the principle of virtual work, which is more simplified than the one derived through the Lagrange formulation approach, and is more suitable for real-time control.

4.3. Dynamic simulation

Let the moving platform track a helical path described by Equations (71), and calculate the actuator forces through the derived dynamics model. We compare the actuator forces generated by the two dynamics models derived through the two different approaches mentioned above, and the deviation can be calculated by

$$\delta f = [(f_{pvw} - f_{Lag})/f_{Lag}] \times 100\% \tag{81}$$

where f_{Lag} and f_{pvw} denote the actuator forces generated by either Lagrange equation or principle of virtual work.

From the simulation results shown in Figure 8, we can see that there is a deviation between the two dynamics models since we introduce a simplifying hypothesis in the second approach, but the deviation is not very large especially when α is larger than 20° where δf is within the range of $\pm 5\%$. And this result demonstrates that the introduced simplifying hypothesis is reasonable.

https://doi.org/10.1017/S0263574704000797 Published online by Cambridge University Press

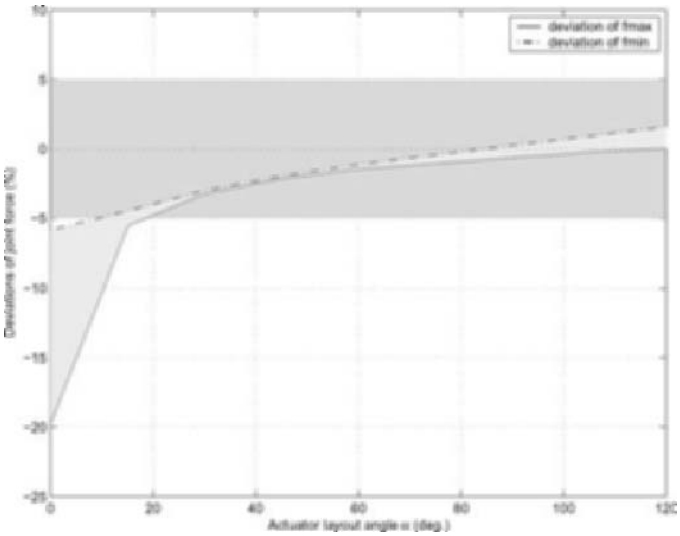


Fig. 8. Force deviation of two dynamics models.

5. CONCLUSIONS

In this paper, the kinematics and inverse dynamics analysis for a general 3-PRS spatial parallel mechanism has been presented. Closed form solutions for the inverse kinematics problem are derived. The forward kinematics problem of a general 3-PRS parallel mechanism is resolved by using Newton iterative numerical method. An illustrated numerical example shows that an acceptable solution can be reached after a few iterations when using the Newton method, providing that an initial guess is closed enough to the actual solution. The kinematics analysis has laid a good foundation for the dynamics analysis.

The dynamics model of a general 3-PRS parallel mechanism is established through two approaches: Lagrange equation and principle of virtual work. By expressing the kinetic and potential energy of all the components of a general 3-PRS parallel mechanism in terms of the chosen generalized coordinates, we derive the dynamic model using the first type of Lagrange's equation. The simulation results of two cases of study quantitatively from viewpoint of conservation of energy and qualitatively from viewpoint of doing work show the validity of the derived dynamics model. By introducing a simplifying hypothesis, the dynamics model of a general 3-PRS parallel mechanism is derived by means of the principle of virtual work, which is more simplified than the one derived by Lagrangian equation. The moving platform is commanded to track a helical path, and the actuator forces are calculated with the two dynamics models. By comparing the actuator forces calculated through the two dynamics models, we can see that the efficiency of the adopted hypothesis can simplify the dynamic model greatly, and the derived dynamics model can be more suitable for real time control. The study presented here provides a sound basis for the future research work on the kinematics and dynamics control of a general 3-PRS parallel mechanism. Moreover the modeling methods and valid verification approaches presented in this paper can also be applied to other parallel mechanisms with less DOF.

Acknowledgments

The authors appreciate the fund support from the research committee of University of Macau under grant no.: RG004/03-04S/LYM/FST and RG024/03-04S/LYM/FST.

References

1. J.-P. Merlet, "Direct Kinematcis of Parallel Manipulators," *IEEE Trans. on Robotics and Automation* **9**(6), 842–845 (1993).
2. K. Harib and K. Srinivasan, "Kinematic and Dynamic Analysis of Stewart Platform-Based Machine Tool Sturctures," *Robotica* **21**, Part 1, 541–554 (1989).
3. R. Clavel, "DELTA, a Fast Robot with Parallel Geometry," *Proc. of 18th International Symposium on Industrial Robot*, Lausanne (1988) pp. 91–100.
4. L. W, Tsai, G. C. Walsh and R. E. Stamper, "Kinematics of a Novel Three DOF Translational Platform," *Proc. of the IEEE Conf. on Robotics and Automation* (1996) **Vol. 4**, pp. 3446–3451.
5. K.-M. Lee and S. Arjunan, "A Three-Degrees-of-Freedom Micromotion in-Parallel Actuated Manipulator," *IEEE Trans. on Robotics and Automation* **7**(5), 634–641 (1991).
6. J. Wang and C. M. Gosselin, "Static Balancing of Spatial Three-Degree-of-Freedom Parallel Mechanism," *Mechanism and Mechine Theory* **34**(3), 437–452 (1999).
7. F. Pierrot and O. Company, "H4: a New Family of 4-DOF Parallel Robots," *Proc. of the IEEE/ASME Conf. on Advanced Intelligent Mechatronics* (1999) pp. 508–513.
8. J. A. Carretero, R. P. Podhorodeski, M. A. Nahon and C. M. Gosselin, "Kinematic Analysis and Optimization of a New Three Degree-of-Freedom Spatial Parallel Manipulator," *ASME J. Mechanical Design* **122**(1), 17–24 (2000).
9. M.-S. Tsai, T.-N. Shiau, Y.-J. Tsai and T.-H. Chang, "Direct Kinematic Analysis of a 3-PRS Parallel Mechanism", *Mechanism and Machine Theory* **38**(1), 71–83 (2003).
10. A. Codourey, "Dynamic Modeling and Mass Matrix Evaluation of the DELTA Parallel Robot for Axes Decoupling Control," *Proc. of the IEEE/RSJ Conf. on Intelligent Robots and Systems* (1996) **Vol. 3**, pp. 1211–1218.
11. K. M. Lee and D. K. Shah, "Dynamic Analysis of a Three-Degree-of-Freedom in-Parallel Actuated Manipulator," *IEEE J. Robotics and Automaton* **4**(3), 361–367 (1988).
12. M. S. Tsai and W. H. Yuan, "Dynamic Analysis of a 3 PRS Parallel Mechanism," *Proc. of 12th National Symposium on Automation, Taiwan* (2001) No. 4303C-1, pp. 1–8.
13. Y.-W. Li, J.-S. Wang, L.-P. Wang and X.-J. Liu, "Inverse Dynamics and Simulation of a 3-DOF Spatial Parallel Manipulator," *Proc. of the IEEE Conf. on Robotics and Automation* (2003) pp. 4092–4097.
14. L. W. Tsai, *Robot Analysis: The Mechanics of Serial and Parallel Manipulator* (John Wiley & Sons, New York, USA, 1999).
15. Y. Li and Q. Xu, "Kinematics and Stiffness Analysis for a General 3-PRS Spatial Parallel Mechanism", *15th CISM-IFToMM Symposium on Robot Design, Dynamics and Control*, Montreal, Canada, (June 14–18, 2004) Romo4–15.

https://doi.org/10.1017/S0263574704000797 Published online by Cambridge University Press